First solar cells on silicon wafers doped using sprayed boric acid

2010 Semicond. Sci. Technol. 25 115012

(http://iopscience.iop.org/0268-1242/25/11/115012)

Semicond. Sci. Technol. **25** (2010) 115012 (4pp) doi:10.1088/0268-1242/25/11/115012

First solar cells on silicon wafers doped using sprayed boric acid

J A Silva[1,3], Miguel C Brito[2], Ivo Costa[1], Jorge Maia Alves[1], João Serra[1] and António Vallêra[1]

[1] Faculty of Sciences, University of Lisbon Campo Grande, Lisbon, Portugal
[2] IDL, University of Lisbon, Lisbon, Portugal

E-mail: jose.almeida-silva@insa-lyon.fr

Received 27 July 2010, in final form 19 September 2010
Published 15 October 2010
Online at stacks.iop.org/SST/25/115012

Abstract
A new method for boron bulk doping of silicon ribbons is developed. The method is based on the spraying of the ribbons with a boric acid solution and is particularly suited for silicon ribbons that require a zone-melting recrystallization step. To analyse the quality of the material thus obtained, multicrystalline silicon samples doped with this doping process were used as substrate for solar cells and compared with solar cells made on commercial multicrystalline silicon wafers. The values obtained for the diffusion length and the *IV* curve parameters show that the method of doping with the boric acid solution is suitable to produce p-doped silicon ribbons for solar cell applications.

1. Introduction

One possible strategy for the cost reduction of silicon solar cells is to reduce the quantity of the semiconductor material used. The growth of silicon crystal directly in the shape of a ribbon or sheet [1] is an interesting approach to reduce the use of silicon feedstock as it avoids the wafering step and its associated kerf loss [2]. Among the many different proposals for the growth of silicon sheets for photovoltaic application [2] there are those that require the use of a recrystallization step, in order to improve the material quality [3, 4].

In this paper we report on the first solar cells produced using a bulk doping technique based on the spraying of the silicon ribbon with a boric acid solution followed by a zone-melting recrystallization (ZMR) step. This technique is particularly suitable to dope silicon ribbons that during their growth require a ZMR step anyway [5–7]. The overall energy budget is therefore unaltered.

The method presented here is compatible with an inline transport system; it also proved to be reliable, safe and easily controllable, and uses an inexpensive and widely available doping source.

[3] Present address: INL, Université de Lyon, INSA, Bât. Blaise Pascal, Villeurbanne, France.

2. Experimental details

Figure 1 describes schematically the process steps of the sprayed boric acid (SBA) doping method. The doping process begins with the cleaning of the sample with a polish solution (75% HNO_3, 15% H_2O+HF, 10% CH_3COOH) and a diluted solution of hydrofluoridric acid. The following step is the deposition of a boric acid solution on the surface of the sample. The boric acid solution is sprayed using an airbrush Badger 250 fed with a constant pressure of nitrogen. After drying, the sample is introduced into a furnace where it is subjected to ZMR in an argon atmosphere.

As the temperature of the sample increases, with the approach of the molten zone, several physical and chemical reactions occur. At 100 °C all the water deposited with the boric acid evaporates, and it is removed from the chamber by argon circulation. As the temperature further increases, the boric acid is dehydrated, thus forming metaboric acid (HBO_2) and boron oxide (B_2O_3) according to the equations [8]

$$H_3BO_3 \rightarrow HBO_2 + H_2O, \quad (1)$$

$$2HBO_2 \rightarrow B_2O_3 + H_2O, \quad (2)$$

$$3H_3BO_3 \rightarrow B_2O_3 + 3H_2O. \quad (3)$$

For a temperature of 450 °C the only substance that remains on the surface of the sample is liquid boron oxide.

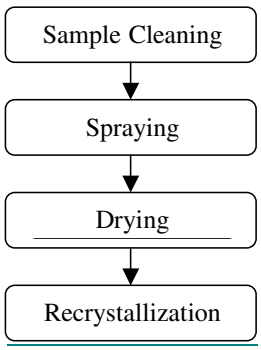

Figure 1. Doping method process steps.

The vapour pressure of boron oxide increases rapidly with temperature, and at 900 °C its evaporation becomes relevant [9]. At this temperature the diffusion of boron atoms into the sample (equation (4)) also becomes important:

$$2B_2O_3(l) + 3Si(s) \rightarrow 3SiO_2(s) + 4B(s). \quad (4)$$

For temperatures over 900 °C there is a competition between the evaporation of boron oxide and the diffusion of boron [6]. When the temperature reaches 1200 °C all the boron oxide is evaporated, thus preventing any further diffusion. When the fusion temperature of silicon is reached all the boron diffused into the sample will dissolve in convecting liquid silicon and will thus be uniformly incorporated along the depth of the sample [10].

After recrystallization the sample is cleaned in a diluted solution of HF, and boron incorporation is monitored measuring the sheet resistivity using a four-point probe.

In order to test the suitability of the SBA doping method for photovoltaic application, a set of solar cells was prepared on samples doped using the SBA method. The original material was highly resistive (>1000 Ω cm) off-spec multicrystalline silicon wafers from Deutsche Solar. These samples are known to be significantly contaminated with iron and with traces of chromium and aluminium [7]. Standard multicrystalline silicon wafers from Silso were used (typical resistivity of 0.5–2 Ω cm) as control samples. In order to discriminate the effect of the SBA doping method itself from the impact of the recrystallization step, a second set of control solar cells were produced on recrystallized multicrystalline silicon solar cells from Silso (typical resistivity of 0.5–2 Ω cm; no extra boron incorporation during the recrystallization step). A total of 16 solar cells were prepared in this study. The solar cell processing of the three sets of samples was run in parallel.

Prior to solar cell formation, SBA samples were characterized by infrared absorption spectra using a spectrophotometer Philips Pye-Unicam SP3-200. The effective carrier lifetime of the minority carriers was measured for the three sets of samples by microwave photoconductance (Semilab WT-1000).

Solar cell preparation for material characterization was then realized. The junction was formed by phosphorus diffusion from a solid source. After mesa etching, a grid of Ti/Pd/Ag front contacts and aluminium back contacts were deposited by vacuum thermal evaporation, followed by contact annealing. Since the purpose of this study is to compare and understand the effect of the SBA doping method for photovoltaic application and not the development of high-efficiency solar cells, no further optimizations were included in the cell preparation, e.g. anti-reflective coatings, doping optimization, defect passivation or back surface fields.

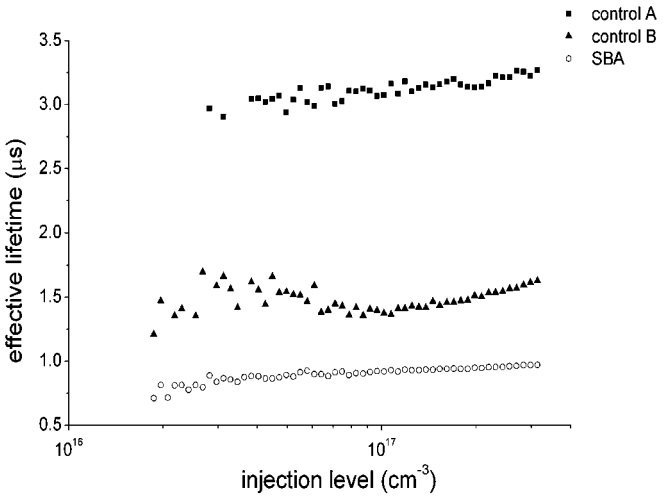

Figure 2. Effective carrier lifetime as function of injection level for non-recrystallized silicon wafer (control A), recrystallized silicon wafer (control B) and SBA sample (SBA).

The solar cells were characterized by measuring spectral response, reflectivity and current–voltage (*IV*) curves.

3. Results

The minority carrier effective lifetime measurements (figure 2) show that the non-recrystallized multicrystalline wafers (control A) feature carrier lifetimes significantly higher than those in both the recrystallized multicrystalline wafers (control B) and the sample doped using the SBA method, both subjected to a ZMR step. It is also observed that control B sample has a higher lifetime than the SBA sample.

In figure 3 the normalized external quantum efficiency (EQE) for the best solar cells of each group is shown. We can observe that the SBA and control B cells have very similar quantum efficiencies, and control A cell has a higher response in the infrared region.

After obtaining the EQE and reflectivity for the three types of cells, the internal quantum efficiency (IQE) was determined. The diffusion length L_e was obtained using the expression [11, 12]

$$RQI^{-1} = 1 + \frac{1}{\alpha L_e},$$

where α is the coefficient of radiation absorption. Results are presented in table 1.

The diffusion length of non-recrystallized control A samples are significantly higher than the diffusion length values of control B and SBA samples.

To characterize the electrical response of the solar cells to light, the *IV* curves were measured under a one-sun

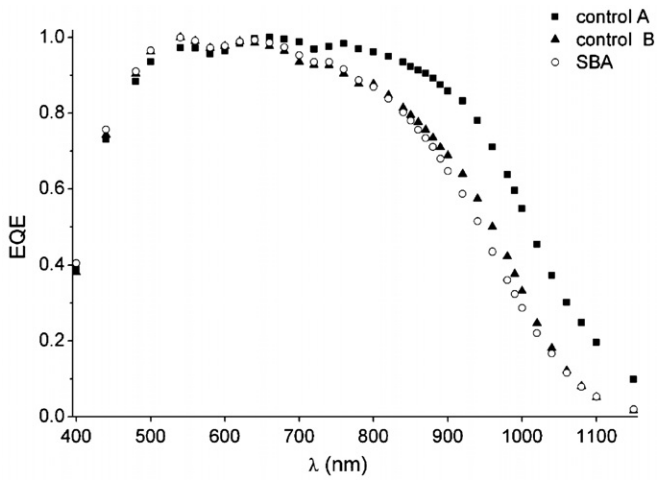

Figure 3. Normalized EQE for non-recrystallized silicon wafer (control A), recrystallized silicon wafer (control B) and SBA sample (SBA).

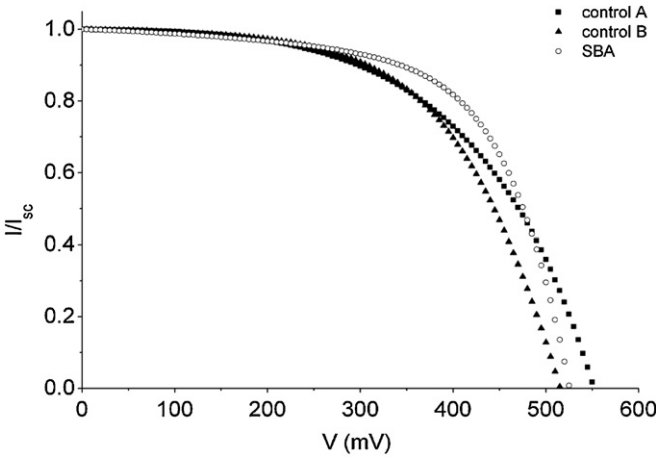

Figure 4. *IV* curves under illumination (normalized) for non-recrystallized silicon wafer (control A), recrystallized silicon wafer (control B) and SBA sample (SBA).

Table 1. Average diffusion length for the three types of cells.

Sample	$L_e(\mu\text{m})$
Control A	131 ± 58
Control B	54 ± 22
SBA	52 ± 17

illumination. Figure 4 shows the *IV* curves for the best solar cell of each of the three groups of cells processed.

Using IVCC, a numerical simulation tool was developed at the University of Konstanz for analysing solar cell *IV* curves [13]; the *IV* curves measured in the dark and under illumination were fitted to the two-diode model with laterally distributed series resistance. The average saturation currents J_{01}, J_{02} and respective standard deviations thus obtained are presented in table 2.

Despite the important standard deviations one can observe that, on average, control B and SBA cells feature higher saturation currents J_{01}, J_{02} than the control A cells. We can also observe that for the SBA cells the saturation current from the base and emitter, J_{01}, is one order of magnitude higher than for the control cells (recrystallized and non-recrystallized). As expected due to the simple and non-optimized solar cell processing, the solar cell performance was rather modest. The best cell reached 5.0% efficiency. Using the *IV* curves under illumination, the values of open circuit voltage (V_{oc}), short-circuit current (J_{sc}), fill factor (FF) and efficiency (η) were obtained. The average cell parameters for the three sets of cells are presented in table 3.

Table 2. Average saturation currents $J_{01,}$ J_{02} for the different types of cells.

Sample	J_{01} (μA cm^{-2})	ΔJ_{01} (μA cm^{-2})	J_{02} (μA cm^{-2})	ΔJ_{02} (μA cm^{-2})
Control A	1.7×10^{-7}	2.9×10^{-7}	0.4	0.2
Control B	4.0×10^{-7}	6.5×10^{-7}	3.4	5.2
SBA	5.1×10^{-6}	3.0×10^{-6}	1.5	1.0

Table 3. Solar cell parameters for the three sets of cells.

Sample	V_{oc} (mV)	J_{sc} (mA cm^{-2})	FF (%)	ΔJ_{02} (μA cm^{-2})
Control A	539 ± 9	16.6 ± 0.8	42 ± 8	3.8 ± 0.9
Control B	468 ± 53	15.1 ± 4.4	50 ± 7	3.5 ± 1.0
SBA	481 ± 40	15.1 ± 3.2	46 ± 11	3.3 ± 0.8

The average cell parameter values show that control A cells have higher performances than control B and SBA cells. It can also be observed that SBA cells have a performance very similar to the control B cells.

4. Discussion

Non-recrystallized control A samples have carrier lifetimes higher than the recrystallized control B and SBA samples. Similarly, solar cells made on non-recrystallized control A samples have diffusion lengths significantly higher than the cells made on control B and SBA samples. We can thus conclude that samples that underwent a recrystallization step have higher recombination rates. This result was expected considering that the density of lattice dislocations increases significantly after recrystallization by zone melting [14, 15] and that dislocations act like recombination centres [16] that are associated with low carrier lifetimes [17, 18].

It is interesting to note that although SBA samples have lower lifetimes than recrystallized control B samples, the diffusion lengths of the solar cells made on these two types of samples are very similar. The lower lifetime in SBA samples may be attributed to high concentration of iron in the original material, as mentioned above. The relative improvement of the diffusion length of SBA samples during solar cell processing may be attributed to metal impurities' gettering during the phosphorous diffusion step [19, 20]. This effect leads to the diffusion of Fe atoms from the base to the emitter, reducing the recombination rate in the former and causing the latter to deteriorate.

One further evidence of this effect is the fact that the value of I_{01}, which corresponds to the saturation current

of the base and the emitter of the cell, for SBA cells is one order of magnitude higher than for control sample cells (both recrystallized and non-recrystallized). Since SBA cells and recrystallized control B cells have similar base doping concentrations and diffusion lengths, the base saturation current must also be similar [21], and therefore one may conclude that the higher value of I_{01} is due to a higher emitter saturation current, originated from the concentration of iron in the emitter of these cells. These high saturation currents obtained for SBA cells contributed significantly for lower FF values.

5. Conclusions

The SBA doping method is a new technique for p-type bulk doping of silicon ribbons in processes that include a ZMR step.

Experimental results have shown lower diffusion lengths in the SBA samples. Since recrystallized multicrystalline control samples showed similar degradation this can be attributed to the recrystallization step. Lifetime measurements prior to the solar cell processing were lower in the SBA samples than in the recrystallized control samples owing to the high impurity (Fe) content of the original material. The detrimental effect of iron in the diffusion length is reduced after solar cell processing due to gettering during the phosphorus diffusion step. However, this also leads to the concentration of impurities in the emitter, significantly increasing the saturation current, and thus limiting the FF.

Since the iron detected in these cells was already present in the original material and was not introduced during the doping process we can conclude that the SBA doping method does not limit the performance of the solar cells, and therefore the SBA method has proved its suitability to be used as a doping method for silicon ribbons that require a recrystallization step.

Acknowledgments

This work has been partially supported by FCT grants SFRH/BD/12763/2003 and SFRH/BPD/20660/2004. The authors would also like to acknowledge Deutsche Solar for providing the samples.

References

[1] Buonassisi T *et al* 2006 *Prog. Photovolt., Res. Appl.* **14** 513
[2] McCann M J, Catchpole K R, Weber K J and Blakers A W 2001 *Sol. Energy Mater. Sol. Cells* **68** 135
[3] Evrard O *et al* 1995 *Proc. 21st European Photovoltaic Solar Energy Conf. and Exhibition* p 1352
[4] Pinto C R, Serra J M, Brito M C, Gamboa R, Maia Alves J and Vallêra A M 2006 *Proc. 21st European Photovoltaic Solar Energy Conf. and Exhibition* p 1099
[5] Silva J A, Costa I, Brito M C, Maia Alves J, Serra J M and Vallêra A M 2006 *Proc. 21st European Photovoltaic Solar Energy Conf. and Exhibition* p 1064
[6] Silva J A, Brito M C, Costa I, Maia Alves J, Serra J M and Vallêra A M 2007 *Sol. Energy Mater. Sol. Cells* **91** 1948
[7] Silva J A, Brito M C, Di Sabatino M, Lobato K, Costa I, Maia Alves J, Serra J M and Vallêra A M 2006 *Proc. 23rd European Photovoltaic Solar Energy Conf. and Exhibition* p 1978
[8] Kracek F C, Morey G W and Merwin H E 1938 *Am. J. Sci.* **35A** 143–71
[9] Chase *et al* 1985 *NIST-JANAF Thermochemical Tables* 3rd edn p 179 Journal of Physical and Chemical Reference Data 14)
[10] Silva J A 2009 *PhD Thesis* University of Lisbon
[11] Serra J M 1995 *PhD Thesis* p 179 University of Lisbon
[12] Basore P A 1990 *IEEE Trans. Electron Devices* **37** 337
[13] Fisher B, Fath P and Bucher E 1999 *Proc. 16th European Photovoltaic Solar Energy Conf. and Exhibition* paper VA1.40
[14] Hu S M 1977 *Appl. Phys. Lett.* **31** 53
[15] Karoui A, Zhang R, Rozgonyi G A and Ciszek T F 2002 *NREL 12th Workshop on Crystalline Silicon Solar Cell Materials and Processes* p 227
[16] El Ghitani H and Martinuzzi S 1989 *J. Appl. Phys.* **66** 1717
[17] Kieliba T, Riepe S and Warta W 2006 *J. Appl. Phys.* **100** 063706
[18] Donolato C 1984 *J. Appl. Phys.* **84** 2656
[19] Gösele U M and Tan T Y 1991 *Mater. Sci. Technol.* **4** 197
[20] Myers S M, Seibt M, Schröter W and Kieliba T 2000 *J. Appl. Phys.* **88** 3795
[21] Goetzberger A, Knobloch J and Voss B 1998 *Crystalline Silicon Solar Cells* (New York: Wiley) p 67